

# Supporting Information

## Laser-Induced Phenylation Reaction to Prepare Semiconducting Single-Walled Carbon Nanotube Arrays

Ying Wang<sup>a</sup>, Jiacheng Wang<sup>a</sup>, Chao Ding<sup>a</sup>, Hongjie Zhang<sup>a</sup>, Ran Du<sup>b</sup>, Shuchen Zhang<sup>c</sup>,  
Jinjie Qian<sup>\*a</sup>, Yue Hu<sup>\*a</sup> and Shaoming Huang<sup>\*a,d</sup>

<sup>a</sup> Key Laboratory of Carbon Materials of Zhejiang Province, College of Chemistry and  
Materials Engineering, Wenzhou University, Wenzhou 325000, P. R. China

<sup>b</sup> Physical Chemistry, Technische Universität Dresden, Bergstrasse 66b, Dresden 01062,  
Germany

<sup>c</sup> Materials Sciences Division, Lawrence Berkeley National Laboratory, Berkeley,  
California 94720, United States.

<sup>d</sup> School of Materials and Energy, Guangzhou Key Laboratory of Low-Dimensional  
Materials and Energy Storage Devices, Guangdong University of Technology,  
Guangzhou 510006, P. R. China

\*Corresponding author

E-mail: yuehu@wzu.edu.cn; jinjieqian@wzu.edu.cn; smhuang@gdut.edu.cn

## **1 Materials**

ethanol (99.5%, aladdin), benzoyl peroxide (BPO, aladdin), acetone (99.7%, aladdin), HF (40%, aladdin). isopropanol (99.7%, aladdin), ultrapure water ( Millipore Co, USA), polymethyl methacrylate (PMMA) (950 K, Allresist), 300 nm-SiO<sub>2</sub>/Si (Hefei Kejing Materials Technology Co), Au, Cr (99.99%, China New Metal Materials Technology CO, Ltd.), Ar, H<sub>2</sub> (99.9%, Zhejiang Haitian gas co. LTD).

## **2 Instruments**

Transmission electron microscopy (TEM, The JEOL JEM-2100F microscope at 200 kV), Tapping-mode AFM (NanoScope IIIa, Veeco Co., USA), Scanning electron microscopy (SEM, Nova 200 NanoSEM, America, operated at 1.0 kV), Raman spectroscopy (Renishaw in via, England) and Keithley 4200-SCS semiconducting Characterization System, Optical Microscope (DM4000M, Leica Microsystems Wetzlar GmbH, Germany), Glue machine (KW-4A/5, Institute of Microelectronics of Chinese Academy of Sciences), Specimen (heating holder HENTING PLATE-250, MTI Corporation), Ceramic fiber muffle furnace (TXC6, Beijing pilemet technology co. LTD), Electron beam evaporation coating machine (JSD500, Anhui jiashuo vacuum technology co. LTD), Ultrapure water machine (Elix5-Milli-Q Academic, Millipore Co, USA), Ultraconication (Scientz SB-5200DTDN, 300 W, 40 kHz). 532nm laser (MGL-III-532, Changchun New Industries Optoelectronics Tech Co. China)

### 3 Experimental section

**Growth of horizontally aligned SWNTs.** In particular, the ST-cut quartz substrates (miscut angle  $<0.5^\circ$ ) are commercially purchased from Hefei Kejing Materials Technology Co., China, which are further annealed at 1000 °C in air for 10 h for better crystallization. The 0.05 mmol/L  $\text{Fe}(\text{OH})_3$  ethanol solution is loaded onto the above quartz substrates. Place the quartz substrate loaded with iron species in the center of a CVD furnace with a 1 inch tube and heat to 830 °C from room temperature in 30 min. 300 standard cubic centimeters per minute (sccm) Ar is continuously introduced to preclude the air and protect the system. After that, 300 sccm hydrogen is purged for 10 min, and then argon through an ethanol bubbler (30 sccm) is introduced for the growth of SWNT arrays at the same temperature of 830 °C for another 30 min. Then, the as-obtained sample is cooled down to room temperature under the protection of argon.

**Phenylation reaction of SWNTs.** BPO molecules is adsorbed by submerging these as-obtained SWNTs into a 0.5 mM BPO isopropanol solution for 30 min, which are dried by a nitrogen flow. Then phenylation of SWNTs is conducted under the laser irradiation (Renishaw in Via-Reflexh, 532 nm excitation wavelength) with the power density of 300 W/cm<sup>2</sup> and the irradiation time is 60 s. Finally, these as-phenylated SWNTs are further inserted into isopropanol for 30 min in order to remove the residual BPO molecules adsorbed and also dried by a nitrogen flow.

**Fabrication of SWNTs FETs.** The  $\text{SiO}_2/\text{Si}$  substrates (300 nm  $\text{SiO}_2$ ) are commercially purchased from Hefei Kejing Materials Technology Co., China. The as-grown SWNTs on quartz are transferred from quartz to a  $\text{SiO}_2/\text{Si}$  substrate through poly-methyl-

methacrylate (PMMA) and 10% mass concentration HF solution. Electrodes are patterned by Electron beam lithography with a channel length of 4  $\mu\text{m}$ . Cr (5 nm)/Au (60 nm) were deposited by thermal evaporation under high vacuum.

**Characterization of SWNTs.** The morphology observation of SWNTs is conducted by SEM (Nova 200 NanoSEM, America, operated at 1.0 kV), and TEM (JEOL JEM-2100F microscope at 200 kV) and tapping-mode AFM (NanoScope IIIa, Veeco Co., USA). Raman spectroscopy (Renishaw in Via-Reflexh) are performed under different laser wavelengths 488, 532, 633 and 785 nm. Keithley 4200-SCS semiconducting characterization system are used to investigate the structures and properties of SWNTs.

### **Acknowledgements**

This work is financially supported by National Natural Science Foundation of China (51972237, 51672193, 51920105004), Natural Science Foundation of Zhejiang Province (LY19E020008), Basic Science and Technology Research Project of Wenzhou (G20190001). We also acknowledge the financial support of Excellent Youth Cultivation Project from Wenzhou University.

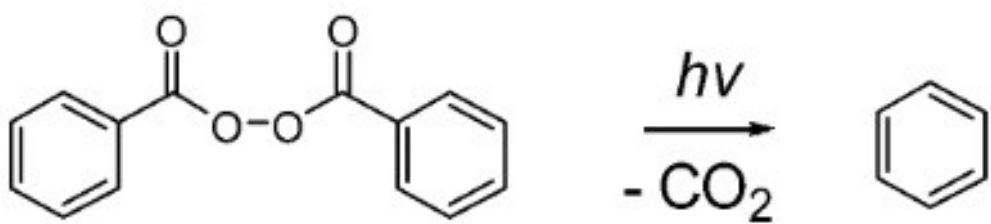


**Fig S1.** Schematic illustration of BPO decomposition to give phenyl radical.

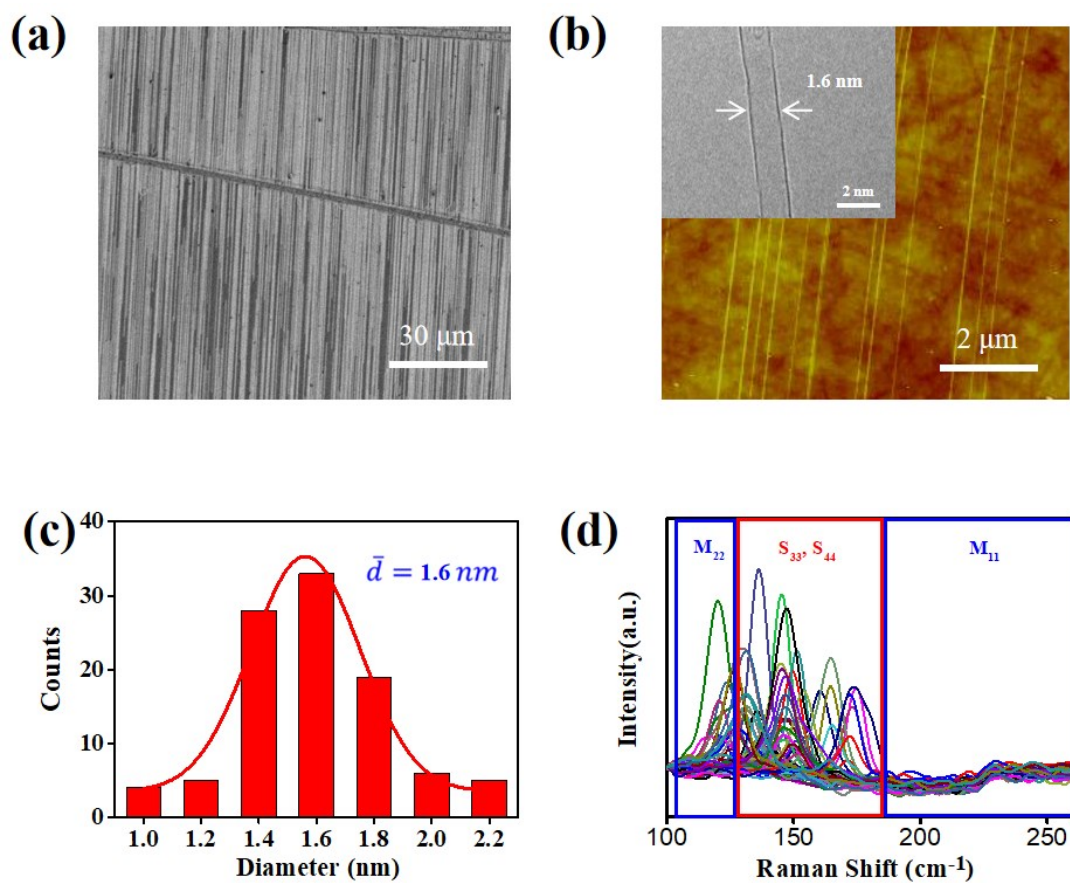


**Fig S2.** (a) SEM images of the as-grown SWNT arrays on quartz surface. (b) AFM images of the as-grown SWNT arrays on quartz surface (inset: TEM image of the as-grown SWNT transferred to the TEM grids). (c) The diameter distribution of the SWNT arrays. (d) Raman spectra of the as-grown SWNT arrays transferred onto the SiO<sub>2</sub>/Si substrate with 532 nm excitation.

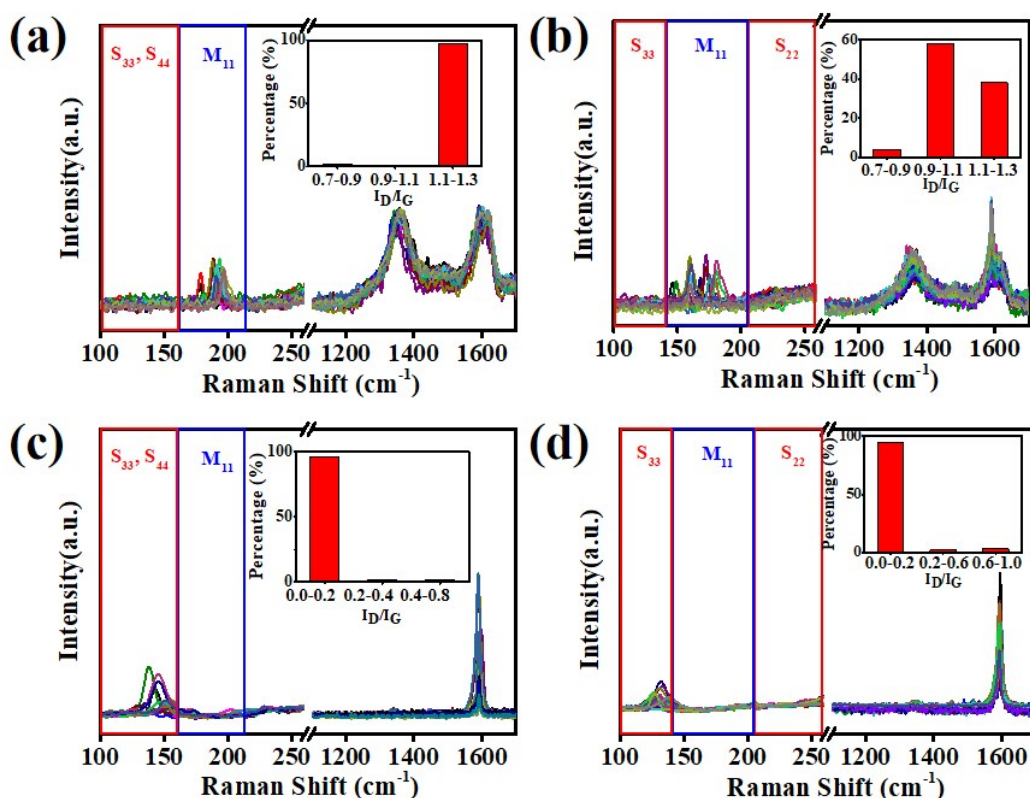


**Fig S3.** (a, c) Raman spectra with 633 nm excitation of m-SWNTs and s-SWNTs after phenylation, respectively. (inset: the statistical result of the  $I_D/I_G$  ratio of m-SWNTs and s-SWNTs after phenylation). (b, d) Raman spectra with 785 nm excitation of m-SWNTs and s-SWNTs after phenylation, respectively. (inset: the statistical result of the  $I_D/I_G$  ratio of m-SWNTs and s-SWNTs after phenylation).

**Fig S3a, 3c** shows the Raman spectra with 633 nm excitation for m-SWNTs after phenylation. A total of 19 RBM signals of the m-SWNTs after phenylation are collected, in which the ratio of the D band and G band ( $I_D/I_G$ ) is calculated to be 1.1-1.3 (97%), 0.9-1.1 (1%) and 0.7-0.9 (2%). And 16 RBM signals of the s-SWNTs after phenylation are collected, in which the  $I_D/I_G$  value is calculated to be 0-0.2 (96%), 0.2-0.4 (2%) and 0.4-0.8 (2%).

**Fig S3b, 3d** shows the Raman spectra with 785 nm excitation for m-SWNTs after phenylation. A total of 26 RBM signals of the m-SWNTs after phenylation are collected, in which the  $I_D/I_G$  ratio is calculated to be 1.1-1.3 (38%), 0.9-1.1 (58%) and 0.7-0.9 (4%). And 21 RBM signals of the s-SWNTs after phenylation are collected, in which the  $I_D/I_G$  value is calculated to be 0-0.2 (95%), 0.2-0.6 (2%) and 0.6-1.0 (3%).



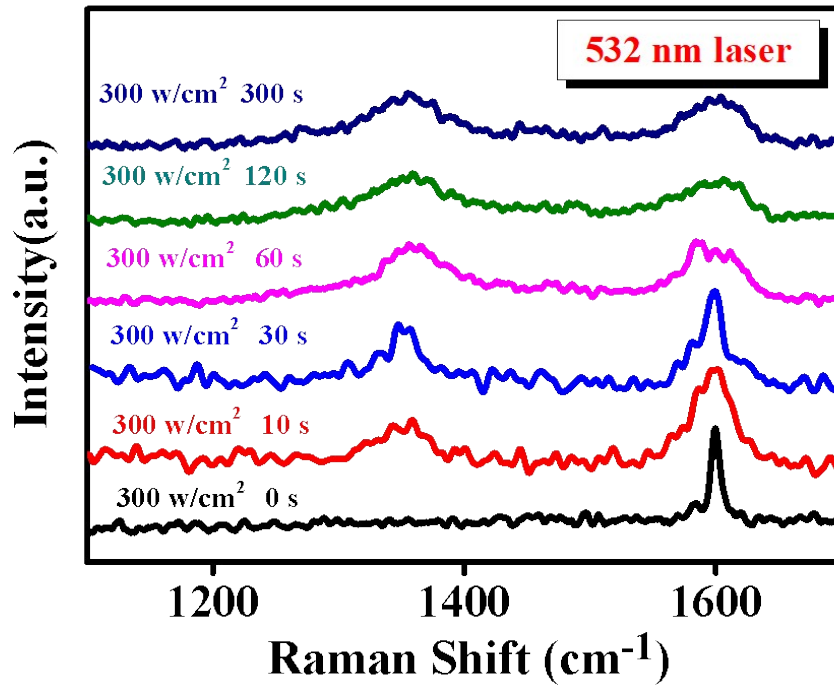


**Fig S4.** Raman spectra with 532 nm excitation of the single m-SWNT with increasing the irradiation time when power density is 300 W/cm<sup>2</sup> under 532 nm laser irradiation.

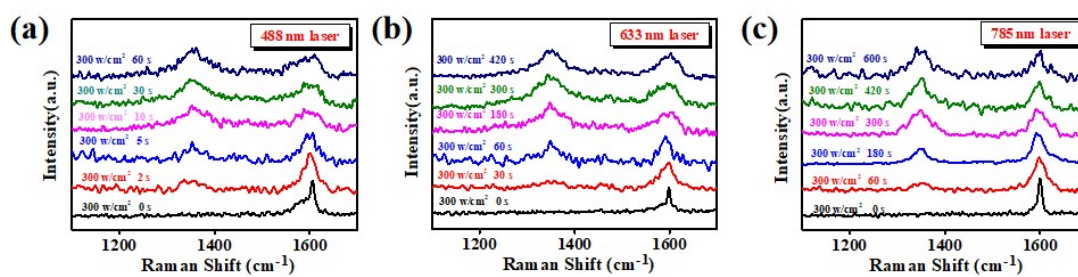


**Fig S5. (a,b,c)** Raman spectra with 532 nm excitation of the single m-SWNT with increasing the irradiation time when power density is 300 W/cm<sup>2</sup> under 488 nm, 633 nm and 785 nm laser irradiation, respectively.

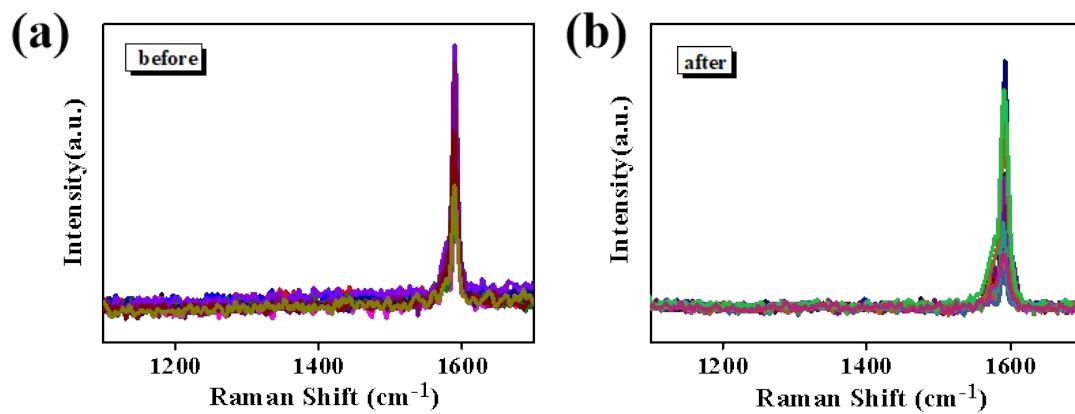


**Fig S6. (a,b)** Raman spectra with 532 nm excitation of SWNT arrays with the absence of BPO molecules before and after phenylation.

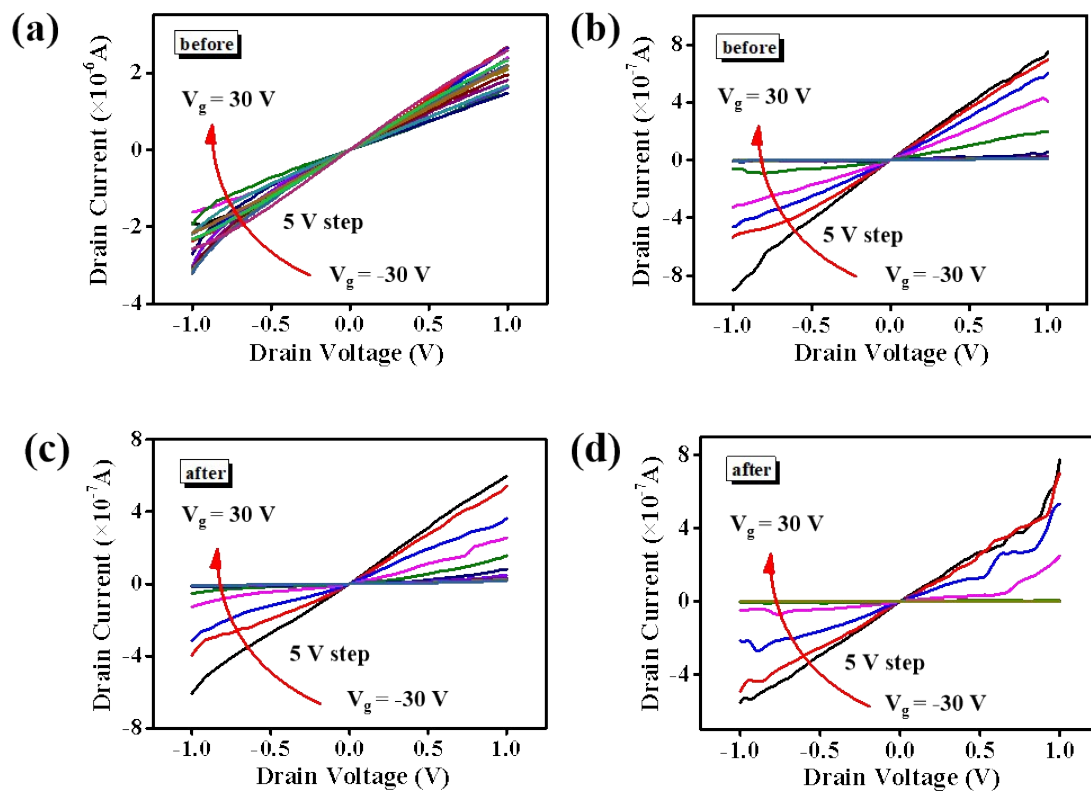


**Fig S7.** (a, c) Typical  $I_{ds}$ - $V_{ds}$  curve of a single m-SWNT-based FET device before and after phenylation. (b, d) Typical  $I_{ds}$ - $V_{ds}$  curve of a single s-SWNT-based FET device before and after phenylation.

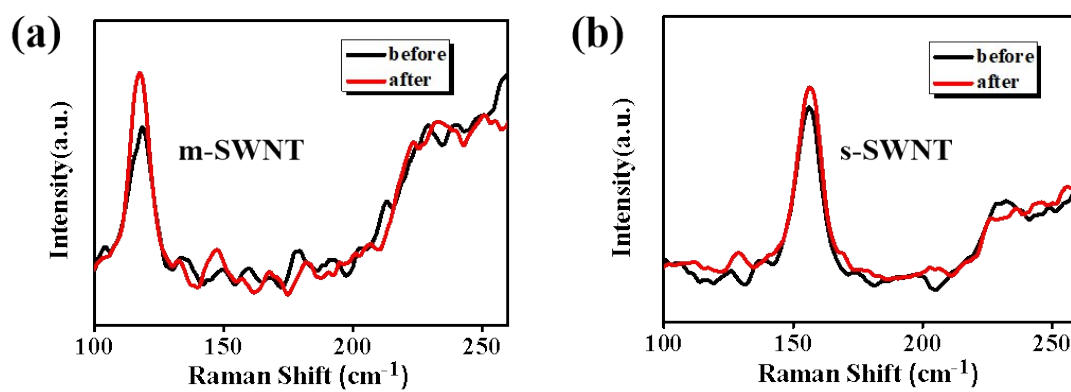


**Fig S8. (a, b)** Raman spectra with 532 nm excitation of m-SWNT and s-SWNT before and after phenylation, respectively.

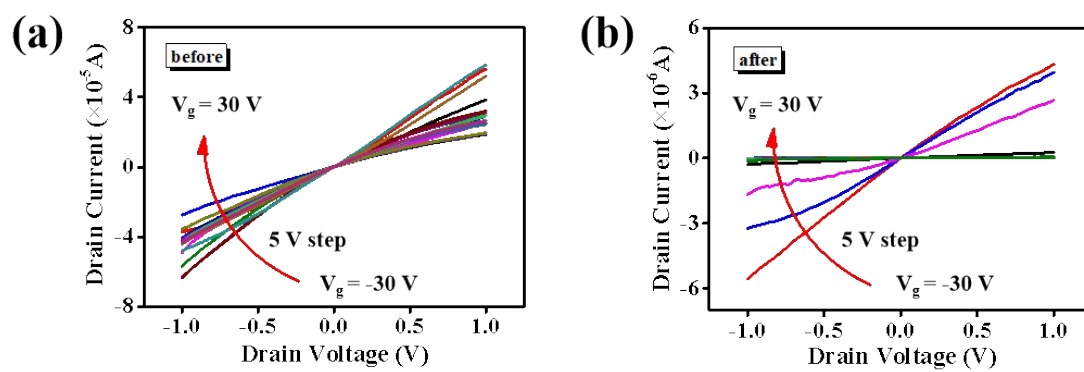


**Fig S9. (a,b)** Typical  $I_{ds}$ - $V_{ds}$  curve of the SWNT-based arrays FET device before and after phenylation.

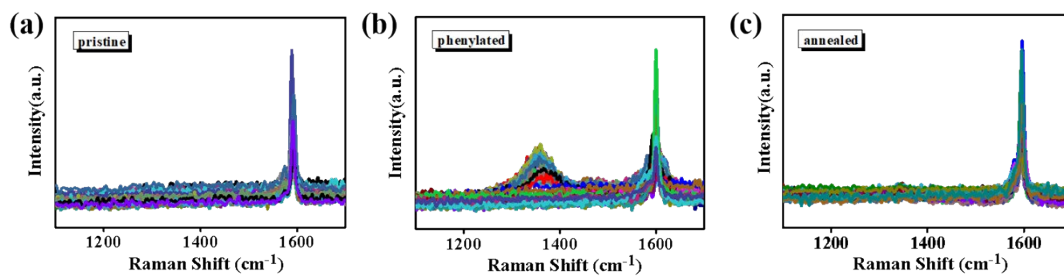


**Fig S10. (a,b,c)** Raman spectra with 532 nm excitation of pristine, phenylated and annealed SWNT arrays.

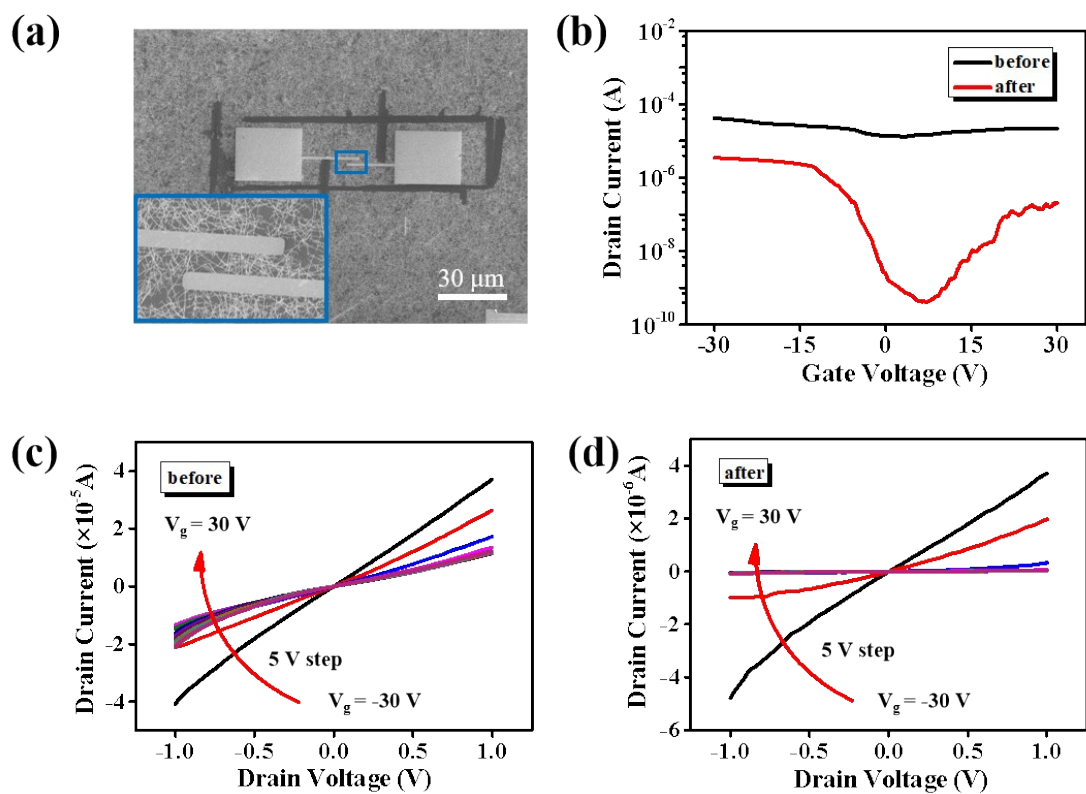


**Fig S11.** (a) SEM image of the SWNT film-based FET device. (b) Typical  $I_{ds}$ - $V_g$  curve of the SWNT film-based FET device at  $V_{ds} = 1$  V before and after phenylation. (c,d) Typical  $I_{ds}$ - $V_{ds}$  curve of the SWNT film-based FET device before and after phenylation.



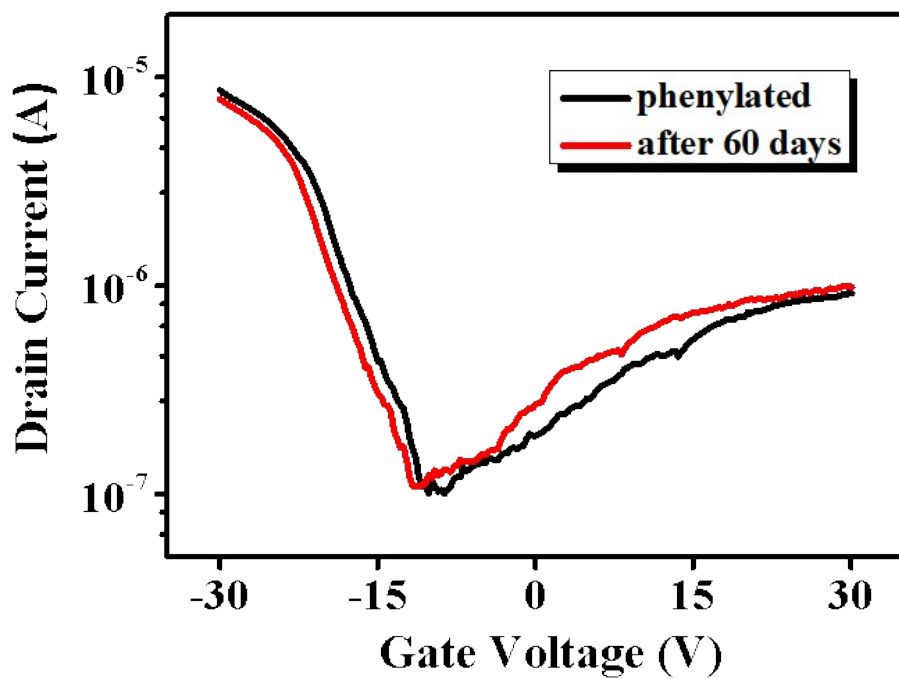


**Fig S12.** Typical  $I_{ds}$ - $V_g$  curves of phenylated SWNT-based arrays FET device before and after 60 days.

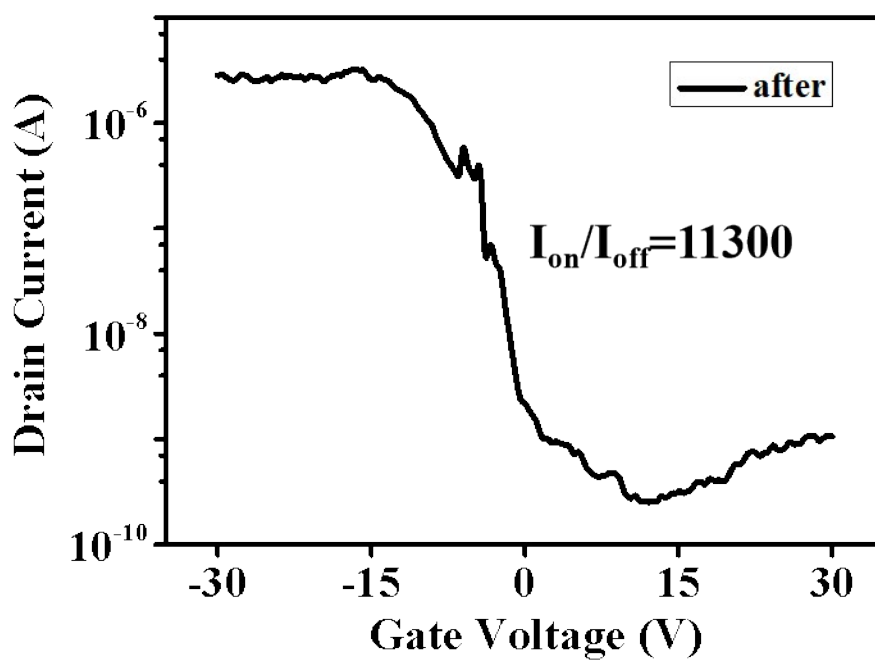


**Fig S13.** Typical  $I_{ds}$ - $V_g$  curves of this champion SWNT arrays-based FET device at  $V_{ds} = 1$  V after phenylation.

**Fig S13** shows typical  $I_{ds}$ - $V_g$  curves of this champion SWNT arrays-based FET device at  $V_{ds} = 1$  V after phenylation, and its  $I_{on}/I_{off}$  ratios is 11300.